Golden Research Thoughts
ISSN 2231-5063
Volume-3, Issue-5, Nov-2013 Available online at www.aygrt.isrj.net

A New Torque Control Method For Torque Ripple Suppression In BLDC Motar With Nonideal Back EMF

Yandamuri Haribabu And V.V. Narasimha Murthy

Department of Electrical and Electronics Engineering, University College of Engineering Kakinada, JNTUK, AP

Abstract— To improve the speed precision and stabilization of the gimbal servo system of double gimbal magnetically suspended control moment gyro, a comprehensive analysis of the reason of electromagnetic torque ripples of BLDC motor with nonideal back electromotive force (EMF) drives in commutation and conduction regions is presented. A novel automatic control method of torque is proposed. With this method. the current control rule is designed, and duty cycle of pulse width modulation (PWM) is regulated by measuring the wave function of back electromotive force. To eliminate the diode freewheeling of inactive phase, the PWM_ON_PWM scheme is used and PI controller is used for the speed regulation. Simulation results are given to show the comparison between HIGH_PWM_L_ON scheme and proposed PWM_ON_PWM scheme, the proposed methos can reduce the torque ripple effectively and improve the speed precision and stabilization as well.

keywords— Brushless direct current (BLDC) motors, electromagnetic torque ripple, nonideal back electromotive force (EMF), double gimbal magnetically suspended control moment gyro (DGMSCMG), pulse width modulation (PWM).

INTRODUCTION

CONTROL moment gyro (CMG) is considered to be one of the primary actuator used for the attitude control of large spacecrafts [1]. The actuator with high-precision, fast-response, and large-angle maneuver characteristics is necessary for the attitude control of spacecrafts. Magnetically suspended control moment gyro (MSCMG) has the advantage of high precision and longevity owing to the zero friction and enhanced damping of high-speed rotor [2]. The gimbal servo system is an important part of Magnetically suspended control moment gyro (MSCMG) and its control precision of angular position and angular speed has severe influence on the properties of the moment output [3]. Brushless direct current (BLDC) motor have characteristics of high reliability, simple frame, and small friction. By comparing with PMSM, BLDC motor has the advantage of high speed adjusting performance and power density [4] [5]. So, the BLDC motor is the ideal choice for the CMG's gimbal system. Therefore, its application in the high precision servo system is restricted due to the electromagnetic torque ripple [6].

The torque ripple reduction and the control performance improvement of BLDC have been the research hotspot in years, and the main research works are focused on commutation torque ripple, the torque ripple produced by diode freewheeling of inactive phase, and the torque ripple caused by the nonideal back electromotive force (EMF). For the commutation torque ripple, Calson *et* al. proposed that relative torque is related to current and varies with speed [7]. In [6], a single dc current sensor and an adaptive phase-change point regulation scheme should be used to suppress the commutation torque ripple, but the diode freewheeling of inactive phase was not considered. Chuang et *al.* have analyzed the influences of different pulse width modulation (PWM) patterns on the commutation torque ripple according to the BLDC motors with unbalanced hall sensors, Speed filter is used to regulate the phase-change point automatically. However, this control method is more competent under the high-speed working condition. In [10], the reasons of commutation torque ripple for low and high speed are analyzed. In order to keep incoming and outgoing phase currents changing at the same rate during commutation, the

duty was regulated at low speed and the dead beat current control was adopted at high speed, but the nonideal back EMF was not considered in this method. It is an effective way to propose some topology circuit for BLDC motor drives to control their dc-link voltage, as shown by some researchers presented in [11] - [13]. In reference [11], a buck converter is used to regulate dc-link voltage to reduce the commutation torque ripple, but the bandwidth of buck converter was not considered, so this structure can only satisfy torque pulsation at low speed. Chen *et* at. Proposed a superlift Luo topology circuit to produce desired dc-lick voltage [12], but this structure is more complex and competent only under high-speed condition. In [13], a SEPIC topology circuit is employed, but this topology structure needs to add three switches and their corresponding inductances, capacitances, and diodes. Here PI controller is used for speed regulation.

For the diode freewheeling of inactive phase, various modulation methods have been analyzed, the PWM_ON_PWM and PWM_PWM methods are considered, which can eliminate the diode freewheeling of inactive phase. Considering the power dissipation PWM_ON_PWM is the better modulation method [14], [15].

In view of torque ripples of BLDC motor with nonideal back EMF, there are mainly two kinds of resolvents. One is to employ direct torque control to regulate current [16]-[19], and the other is to apply the motor's back EMF waveform functions to regulate the current [20]-[23]. In [16], the direct torque control method is adopted, but the back EMF and phase current need to be measured. So, the complexity of the circuit and software is increased. In [18], DSC control method is introduced into the BLDC motor, but the characteristic of nonideal back EMF was not considered.

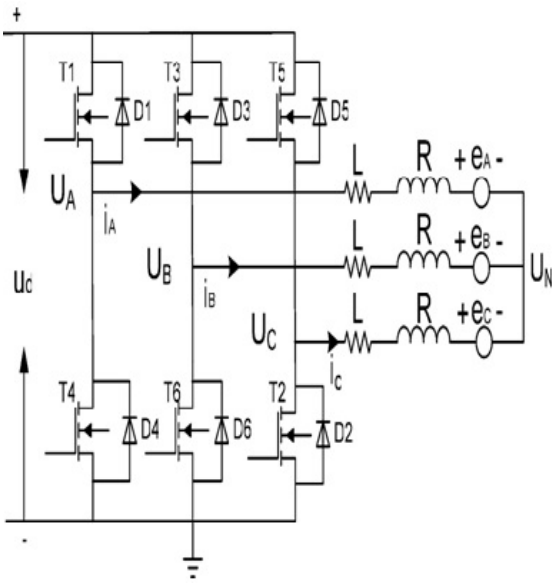

Fig. 1. Block diagram of BLDC drive system.

In [19], a prediction control method was used to obtain reduced switching frequency while keeping torque within the desired hysteresis band. In [20], the influence of high harmonics on the motor's torque was analyzed. In [21], the control method in which the torque ripple can be reduced by changing the dc-link voltage is analyzed and simulated, but the corresponding topology structure was not given. Aghili *et* al. proposed an optimal commutation scheme based on Fourier decomposition with back EMF and estimating the Fourier coefficients to reduce the torque ripple and speed ripple [22], [23]. Lu *et* al. proposed at torque method for minimizing the torque ripple of BLDC motor with nonideal back EMF [24], but the diode freewheeling of the inactive phase was not considered and the modulation scheme is PWM_PWM. For space application, the magnets and the sensors of the BLDC motor are made to tight tolerances, so the manufacturing imprecision is not an issue.

This paper proposed a new current control method for the BLDC motors with nonideal back EMF. In this method, PWM_ON_PWM method is used to eliminate the current through the freewheeling diode when the phase is inactive. The motor's phase current, angular position, and speed are measured in real time and the duty cycle is precalculated in the designed current controller to control the phase current. In addition, commutation time is calculated in the controller. Simulation and experimental results showed that, compared with the conventional current control method, the new control method can reduce the torque ripple effectively.

II. DESIGN OF TORQUE CONTROL METHOD

The BLDC motor is considered as three-phase star connected and is fed by a conventional three-phase voltage source inverter. Its configuration is shown in Fig. 1, where R, L, e, U, i, $U_{N,}$ and U_d represents the armature resistance, inductance, back EMF, terminal voltage, phase current, motor neutral voltage, and dc-link voltage, respectively.

The assumption made for the development of BLDC motor model are: 1) iron and stray losses are neglected; and 2) three-phase winding are symmetrical. The voltage equations of three winding with phase variables are

$$U_A = Ri_A + L\frac{di_A}{dt} + e_A + U_N \quad (1)$$

$$U_B = Ri_B + L\frac{di_B}{dt} + e_B + U_N \quad (2)$$

$$U_C = Ri_C + L\frac{di_C}{dt} + e_C + U_N \quad (3)$$

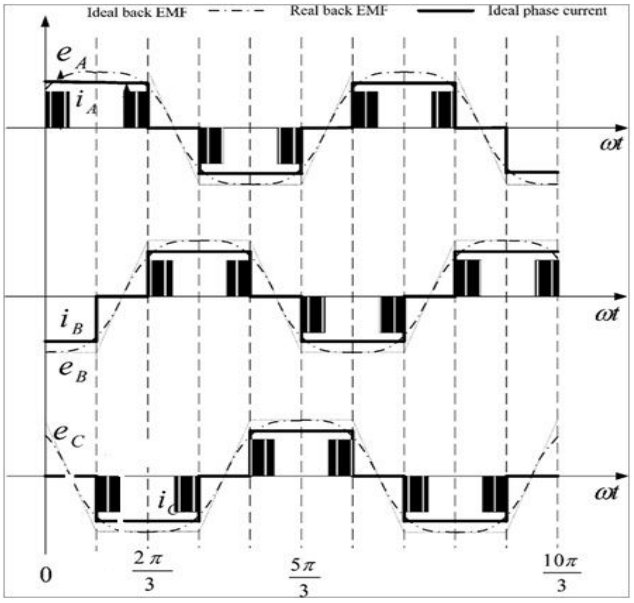

Fig. 2. PWM_ON_PWM pattern

And the equation of the electromagnetic torque is

$$Te = \left(\frac{e_A i_A + e_B i_B + e_C i_C}{\omega}\right) \quad (4)$$

Where T_e is the electromagnetic torque of motor, ω is the mechanical angular velocity of rotor. As three windings are connected as star, the relationship of three-phase current

$$i_A + i_B + i_C = 0 \quad (5)$$

A. Normal Conduction Period

In the $\pi/3 \sim \pi/2$ period, T_1 is switched ON and T_2 is chopping, the current flows into phase A and then out from phase C, $i_A = -i_C$, $i_B = 0$. According to (4), the torque function can be obtained as

$$T_{e1} = \frac{e_A i_A + e_C i_C}{\omega} \quad (6)$$

Assuming the duty cycle of switch T2 is D, the phase voltage equations in the normal conduction period can be described as

$$U_A = Ri_A + L\frac{di_A}{dt} + e_A + U_N = u_d \quad (7)$$

$$U_B = e_B + U_N \quad (8)$$

$$U_C = Ri_C + L\frac{di_C}{dt} + e_C + U_N = (1-D)u_d \quad (9)$$

So, the neutral voltage can be given as

$$U_N = \frac{2u_d - D \times u_d - e_A - e_C}{2} \quad (10)$$

Substituting (10) into (7) and (9), respectively, the current derivation functions of phase A and C are shown as follows:

$$\frac{di_A}{dt} = \frac{D \times u_d + e_C - e_A}{2L} \quad (11)$$

$$\frac{di_C}{dt} = \frac{e_A - e_C - D \times u_d}{2L} \quad (12)$$

As the carrier cycle of PWM is much less than the electrical time constant of stator winding, the effect of motor armature resistance is neglected. Since the sampling time T_s is very short, it is assumed that the sampling time, and the current of phase A and C can be described as

$$i_A(k+1) = \frac{D(k) \times u_d + e_C(k) - e_A(k)}{2L} T_S + i_A(k) \quad (13)$$

$$i_C(k+1) = \frac{e_A(k) - e_C(k) - D(k) \times u_d}{2L} T_S + i_C(k) \quad (14)$$

By combining (13), (14), and (6), the discrete expression of torque in the normal conduction period can be obtained as

$$T(k+1) = T(k) + \frac{D(k)u_d(e_A(k) - (e_C(k)) - (e_A(k) - e_C(k))2}{2L\,\omega(k)} T_S \quad (15)$$

Where T(k+1) is the reference torque T_{ref} of the next period. From (15), the duty cycle D(k), which is the control value of the next period, can be solved as

$$D(k) = \frac{2L\,\omega(k)(T_{ref} - T(k)) + (e_A(k) - (e_C(k))2}{u_d(e_A(k) - e_C(k))T_S} \quad (16)$$

In the $\pi/2 \sim 2\pi/3$ period, switch T2 is ON and T1 is chopping, the current also flows into phase A and out phase C, where $i_A = -i_C$, $i_B = 0$. The three-phase voltage functions are shown follows:

$$U_A = Ri_A + L\frac{di_A}{dt} + e_A + U_N = D \times u_d \quad (17)$$

$$U_B = + e_B + U_N \quad (18)$$

$$U_C = Ri_C + L\frac{di_C}{dt} + e_C + U_N = 0 \quad (19)$$

The neutral voltage function and the current derivative functions of phase A and C are shown as follows:

$$U_N = \frac{D \times u_d - e_A - e_C}{2} \quad (20)$$

$$\frac{di_A}{dt} = \frac{D \times u_d + e_C - e_A}{2L} \quad (21)$$

$$\frac{di_C}{dt} = \frac{e_A - e_C - D \times u_d}{2L} \quad (22)$$

By comparing (21) with (11) and comparing (22) with (12), the duty cycle of the system are same in $\pi/3 \sim \pi/2$ period and $\pi/2 \sim 2\pi/3$ period.

B. Commutation Period

Assuming at a particular commutation process, the current transferring from phase A to B is considered, T1 is switched OFF and T2 is switched ON, T3 is chopping, so the three-phase voltage equations are

$$U_A = Ri_A + L\frac{di_A}{dt} + e_A + U_N = 0 \quad (23)$$

$$U_B = Ri_B + L\frac{di_B}{dt} + e_B + U_N = D \times u_d \quad (24)$$

$$U_C = Ri_C + L\frac{di_C}{dt} + e_C + U_N = 0 \quad (25)$$

From the previous three equations, the neutral voltage can be described as

$$U_N = \frac{D \times u_d - e_A - e_B - e_C}{3} \quad (26)$$

Substituting (26) into (23), (24), and (25), the differential functions of phase current are shown as

$$Ri_A + L\frac{di_B}{dt} = -e_A - U_N = \frac{e_B + e_C - 2e_A - D \times u_d}{3}$$

$$= u_{a1} \quad (27)$$

$$Ri_B + L\frac{di_B}{dt} = D \times u_d - e_B - U_N = \frac{2D \times u_d + e_A + e_C - 2e_B}{3}$$

$$= u_{b1} \quad (28)$$

$$Ri_C + L\frac{di_C}{dt} = -e_C - U_N = \frac{e_A + e_B - 2e_C - D \times u_d}{3}$$

$$= u_{c1} \quad (29)$$

With the initial condition of $i_A(t=0)=I$, $i_B(t=0)=0$, and $i_C(t=0)=-I$, (27) and (28) can be solved as

$$i_A = \frac{u_{a1}}{R} + (I - \frac{u_{a1}}{R})e^{-(\frac{R}{L})t} \quad (30)$$

$$i_B = \frac{u_{b1}}{R} - \frac{u_{b1}}{R}e^{-(\frac{R}{L})t} \quad (31)$$

Expanding $e^{-(\frac{R}{L})t}$ through Taylor series, and neglecting its quadratic term or more. The first-degree term can be derived as $e^{-(\frac{R}{L})t} = 1 - (\frac{R}{L})t$ Substituting it into (30) and (31), the time t_{a1} when i_A decreases from 1 to 0 an the time t_{b1} when i_B increases from 0 to 1 can be solved as

$$t_{a1} = \frac{3IL}{3IR + 2e_A - e_B - e_C + D \times u_d} \quad (32)$$

$$t_{b1} = \frac{3IL}{2D \times u_d + e_A + e_C - 2e_B} \quad (33)$$

If the motor has no commutation torque ripple on the condition working at PWM_ON_PWM scheme, t_{a1} must be equal to t_{b1}, and neglecting the influence of the resistance, the duty cycle of commutation period can be determined as

$$D(k) = \frac{e_A(k) + e_B(k) - 2e_C(k)}{u_d} \quad (34)$$

For 0 < D(k) < 1, it can be deduced from (34) that the commutation torque ripple cannot be restrained through regulating duty cycle of PWM. In (20), overlapping commutation torque ripple. In this method, the switch T1 is still chopping at the time of Δt after phase-change point, and the three-phase voltage equations are

$$U_A = S \times u_d = Ri_A + L\frac{di_A}{dt} + e_A + U_N \quad (35)$$

$$U_B = u_d = Ri_B + L\frac{di_B}{dt} + e_B + U_N \quad (36)$$

$$U_C = (1 - S)\ u_d = Ri_C + L\frac{di_C}{dt} + e_C + U_N \quad (37)$$

Where S1is the switching function and S=1 denote switching ON and S=0 denote switching OFF. In every carrier cycle of PWM, S maintains 1 during D_2T_S and the neutral voltage U_N can be solved from (35), (36), and (37) shown as follows:

$$U_N = \frac{2u_d - e_A - e_B - e_C}{3} \quad (38)$$

Substituting (38) into (35) and (36), the influence of the resistance is neglected, and the differential functions of phase current can be described as

$$L\frac{di_A}{dt} = D_2 \times u_d - e_A - U_N$$

$$= \frac{(3D_2 - 2)u_d + e_B + e_C - 2e_A}{3} = u_{a2} \quad (39)$$

$$Ri_B + L\frac{di_B}{dt} = u_d - eB - U_N$$

$$= \frac{u_d + e_A + e_C - 2e_B}{3} = u_{b2} \quad (40)$$

Similarly the time t_{a2} when i_A decreases form 1 to 0 an the time t_{a2} when i_B increases from 0 to 1 can be solved as (41) and (42) with the same method

$$ta2 = \frac{3IL}{2e_A - e_B - e_C + (3D_2 - 2) \times u_d} \quad (41)$$

$$tb2 = \frac{3IL}{u_d + e_A + e_C - 2e_B} \quad (42)$$

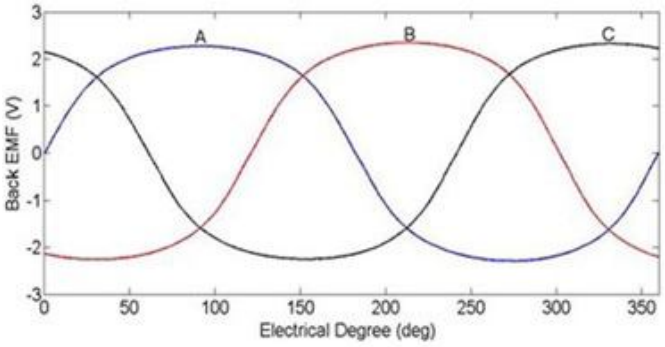

Fig.3. Measured waveform of back EMF

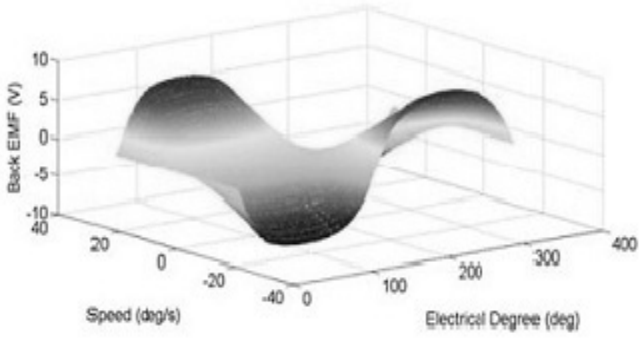

Fig.4.Waveform of angular position, speed and back EMF

So the duty cycle of PWM can be solved as (43) when motor works at medium and high speeds

$$D_2(k) = 1 - \frac{e_A(k) + e_B(k) - 2e_C(k)}{3u_d} \quad (43)$$

C. Measuring Method of Back EMF

Because the back EMF of BLDC motor is proportional to the angular speed, the waveform function can be described as

$$\begin{Bmatrix} e_A(c) = g_A(c) \cdot \omega m \\ e_B(c) = g_B(c) \cdot \omega m \\ e_C(c) = g_C(c) \cdot \omega m \end{Bmatrix} \quad (44)$$

The angular of motor can be measured from the photoelectric encoder fixed on the motor shaft, so the back EMF of every angle can be measured through offline mode. The waveform of three phase back EMF is shown as Fig. 3. As the three-phase winding are symmetrical, the difference between two adjacent phases of back EMF is 120˚ electric angle. So, it is possible to measure the back EMF of phase A only at different speeds, and the corresponding relationship among the motor's angular position, speed, and back EMF are shown as Fig. 4.

III. SIMULATION RESULTS

To verify the feasibility of the proposed current control algorithm, simulations based on conventional current control algorithm and the new current algorithm are carried out for the BLDC motor as follows.

The simulated waveforms using H_PWM_L_ON patters are given in Figs. 5-7. The carrier wave cycle is 20K and the duty cycle is 50%.

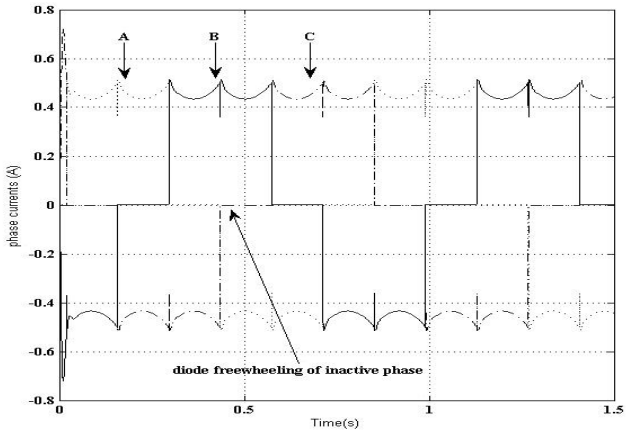

Fig.5. Simulated current using H_PWM_L_ON pattern

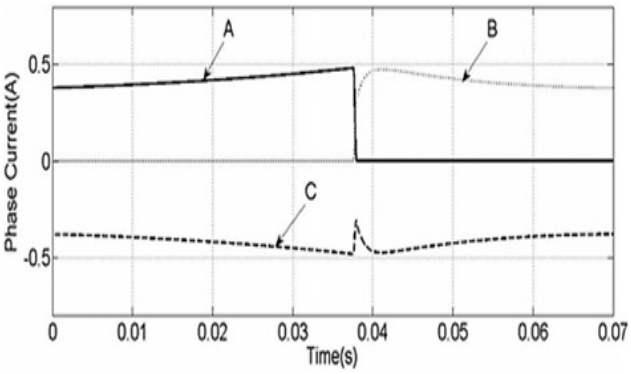

Fig.6. Phase current using H_PWM_L_ON pattern at commutation period

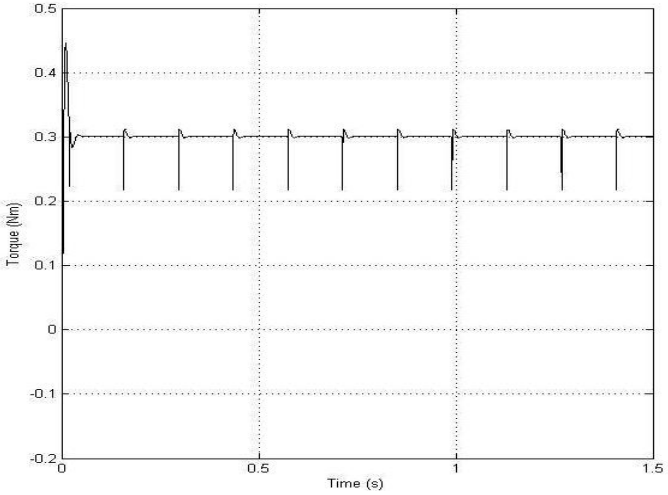

Fig.7. Simulated torque using H_PWM_L_ON pattern

Fig. 5 shows the simulated three-phase current waveform. It shows that the current ripple produced by the non ideal back EMF and changing with commutation exists and there are large current ripples at the phase-change point. Moreover, the current ripples exist on the inactive phase.

Fig. 6 shows three-phase current waveform at the commutation period. During this time, T1 is switched OFF, T3 is switched ON and chopping, and T2 is ON. It shows that the descending rate of phase current A is faster than the rising rate of phase current B, and commutation current ripple is produced on the current of phase C.

Fig. 7 shows the torque waveform using the traditional current control method. in this figure, not only large commutation torque ripple, but also periodic torque ripple produced by the nonideal back EMF change with current commutation.

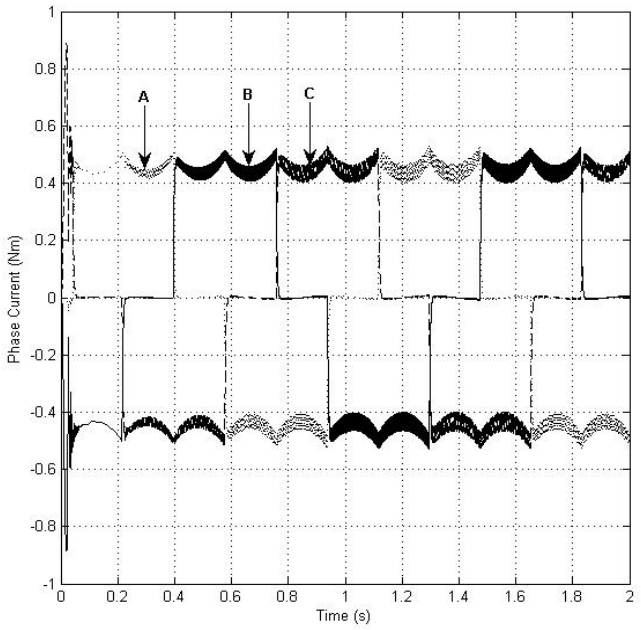

Fig.8. Simulated current using the new current control method in low speed

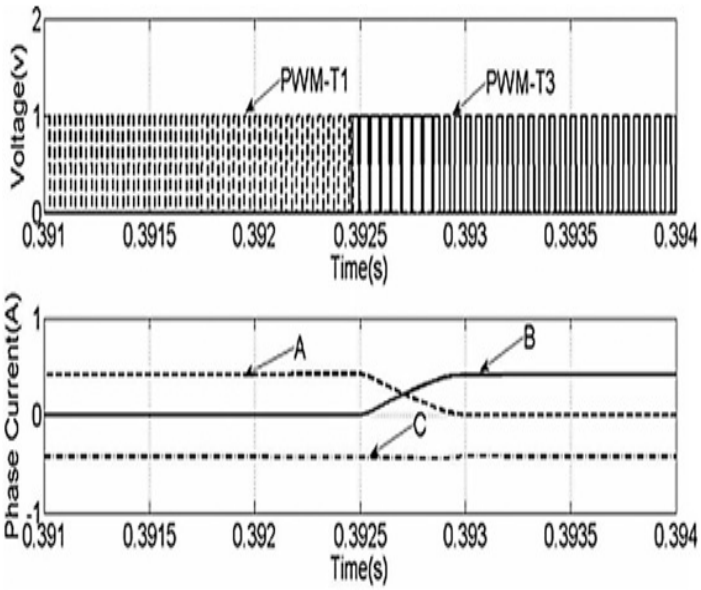

Fig.9. Simulated current and PWM waveform using the new current control method at commutation in low speed

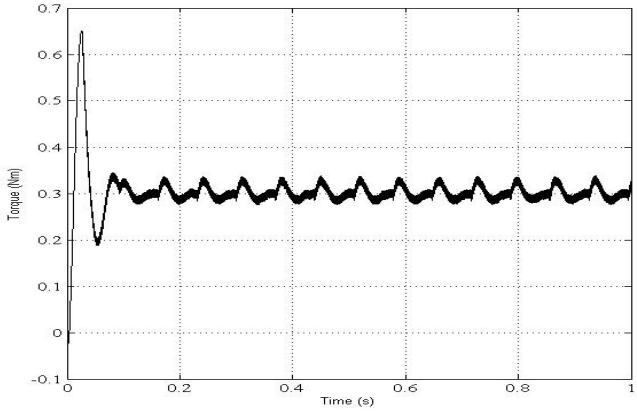

Fig.10. Simulated torque using the new current control method in low speed

The simulated waveform using a new current controller when motor works at low speed are given in Figs. 8-10. Fig. 8 shows the simulated three-phase current waveform. Comparing with Fig. 5, the commutation torque ripple and the diode freewheeling of the inactive phase are eliminated.

Fig. 9 shows the three-phase current waveform and the PWM waveform of switch T1 and T3 at the commutation period. It can be concluded that, when T1 switches OFF and T3 switches ON, the duty cycle of T3 will be increased, and also the current rising rate of phase B will speed up.

So, the current rising rate and the descending rate of phase A are almost equal. There is no ripple on the current of phase C and the commutation torque ripple is eliminated.

Fig. 10 shows the torque waveform of the motor. Comparing with Fig. 7, the torque ripple is smaller using a new current controller on the condition that the output torque is same.

Figs. 8-10 are given to show the simulated waveforms using a new current controller when motor works at low speed.

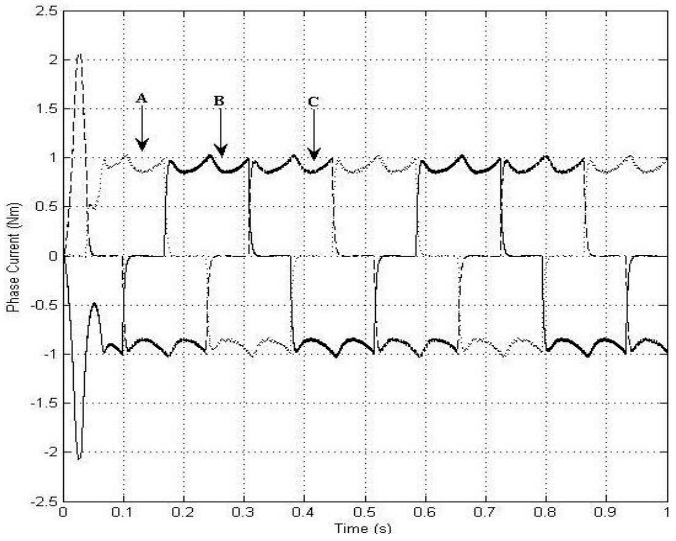

Fig.11. Simulated current using the new current control method in high speed.

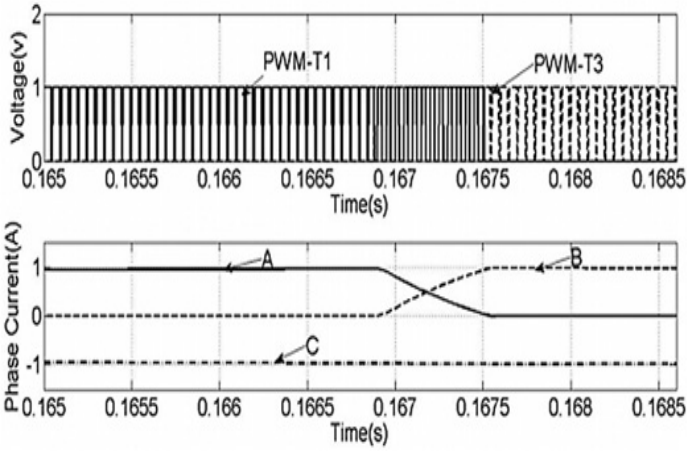

Fig.12. Simulated current and PWM waveform using the new current control method at commutation period with high speed

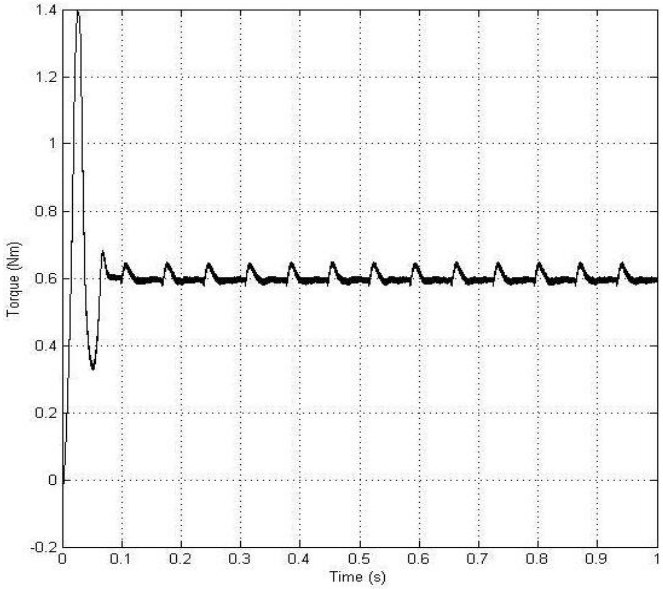

Fig.13. Simulated torque using the new current control method with high speed

In Figs. 11 and 12, it can be seen that, when the motor works at high speed and the current transfers from phase A to phase B, the switch of T1is not OFF and the switch T3 is ON at the phase-change point, and T1 is switched OFF then.

With this method, the current rising rate of phase A is equal to the current descending rate of phase B's current, and the commutation torque ripple is restrained. Fig. 13 shows the conclusion. The torque ripple is 6.3% of the outputting torque at high speed using the new current control scheme.

V. CONCLUSION

In view of the pulsation of three-phase BLDC motor with nonideal back EMF, a new current control method is proposed. The PWM_ON_PWM pattern is used to eliminate the diode freewheeling of inactive phase. When the motor works at low speed, the torque ripple is restrained by speeding up the turn-ON phase current through increasing the duty of PWM. When the motor works at high speed, overlapping commutation scheme is used. The commutation times are given by the current controller in low and high speeds. Aiming at the nonideal back EMF, the duty is calculated in the current controller by measuring the angular position, speed, and the offline measured back EMF. The simulated results carried out on the brushless direct current motor validates the validity of the proposed current control method.

REFERENCES

[1] V. J. Lappas, W. H. Steyn, and C. Underwood, "Design and testing of a control moment gyroscope cluster for small satellites," *J. Spacecraft Rockets*, vol. 42, no. 4, pp. 729–739, 2005.

[2] T. Wei and J. C. Fang, "Dynamics modeling and vibration suppression of high-speed magnetically suspended rotor considering first-order elastic natural vibration," in *Proc. 9th Int. Symp. Magn. Bearings*, 2004.

[3] Z. Wu and J. Y. Zhang, "Dynamics and control of gimbal servo systems for control moment gyroscopes," *J. Basic Sci. Eng.*, vol. 15, no. 1, pp. 130– 136, Jul. 2007.

[4] T.-H. Kim and M. Ehsani, "Sensorless control of the BLDC motors from near-zero to high speeds," *IEEE Trans. Power Electron.*, vol. 19, no. 6, pp. 1635–1645, Nov. 2004.

[5] S. B. Ozturk, W. C. Alexander, and H. A. Toliyat, "Direct torque control of four-switch brushless DC motor with non-sinusoidal back EMF," *IEEE Trans. Power Electron.*, vol. 25, no. 2, pp. 263–271, Feb. 2010.

[6] D. Chen and J. C. Fang, "Commutation torque ripple reduction in PM brushless DC motor with nonideal trapezoidal back EMF," in *Proc. CSEE*, Oct. 2008, vol. 28, no. 30, pp. 79–83.

[7] R. Calson, L.-M. Milchel, and J. C. Fagundes, "Analysis of torque ripple due to phase commutation in brushless dc machines," *IEEE Trans. Ind. Appl.*, vol. 28, no. 3, pp. 632–638, May/Jun. 1992.

[8] H. S. Chuang and Y.-L. Ke, "Analysis of commutation torque ripple using different PWM modes in BLDC motors," in *Conf. Rec. IEEE Ind. Commercial Power Syst. Tech. Conf.*, 2009, pp. 1–6.

[9] N. Samoylenko, Q. Han, and J. Jatskevic, "Dynamic performance of brush-less DC motors with unbanlanced hall sensors," *IEEE Trans. Energy Convers.*, vol. 23, no. 3, pp. 752–763, Sep. 2008.

[10] J. H. Song and I. Choy, "Commutation torque ripple reduction in brushless DC motor drives using a single DC current sensor," *IEEE Trans. Power Electron.*, vol. 19, no. 2, pp. 312–319, Mar. 2004.

[11] X. F. Zhang and Z. Y. Lu, "A new BLDC motor drives method based on BUCK converter for torque ripple reduction," in *Proc. IEEE Power Electron. Motion Control, Conf.*, 2006, pp. 1–4.

[12] W. Chen, C. L. Xia, and M. Xue, "A torque ripple suppression circuit for brushless DC motors based on power DC/DC converters," in *Proc. IEEE Ind. Electron. Appl. Conf.*, 2006, pp. 1–4.

[13] T. N. Shi, Y. T. Guo, P. Song, and C. L. Xia, "A new approach of minimizing commutation torque ripple for brushless DC motor based on DC-DC converter," *IEEE Trans. Ind. Electron.*, vol. PP, no. 99, pp. 1–9, 2010.

[14] K. Wei, C. S. Hu, and Z. C. Zhang, "A novel commutation torque ripple suppression scheme in BLDCM by sensing the DC current," in *36th IEEE Power Electron. Spec. Conf.*, 2005, pp. 1259–1263.

[15] G.W. Meng, X. Hao, and H. S. Li, "Commutation torque ripple reduction in BLDC motor using PWM_ON_PWM mode," in *Proc. Int. Conf. Electr. Mach. Syst. Conf.*, 2009, pp. 1–6.

[16] K. Seog-Joo and S. Seung-Ki, "Direct torque control of brushless DC mo-tor with nonideal trapezoidal back EMF," *IEEE Trans. Power Electron.*, vol. 10, no. 6, pp. 796–802, Nov. 1995.

[17] G. R. A. Markadeh, S. I. Mousavi, and E. Daryabeigi, "Position sensorless direct torque control of BLDC motor by using modifier," in *Proc. 11th Int. Conf. Optim. Elect. Electron. Equipment*, 2008, pp. 93–99.

[18] J. Gao and Y. Hu, "Direct self-control for BLDC motor drives based on three-dimensional coordinate system," *IEEE Trans. Ind. Electron.*, vol. 57, no. 8, pp. 2836–2844, Aug. 2010.

[19] T. Geyer, G. Papafotiou, and M. Morari, "Model predictive direct torque control—Part I: Concept, algorithm, and analysis," *IEEE Trans. Ind. Electron.*, vol. 56, no. 6, pp. 1894–1905, Jun. 2009.

[20] L. Lianbing, J. Hui, Z. Liqiang, and S. Hexu, "Study on torque ripple attenuation for BLDCM based on vector control method," in *Proc. 2th Int. Conf. Intell. Netw. Intell. Syst.*, 2009, pp. 605–608.

[21] K.-Y. Nam, W.-T. Lee, and C.-M. Lee, "Reducing torque ripple of brush-less DC motor by varying input voltage," *IEEE Trans. Magn.*, vol. 42, no. 4, pp. 1307–13210, Apr. 2006.

[22] F. Aghili, M. Buehler, and J. M. Hollerbach, "Optimal commutation laws in the frequency domain for PM synchronous direct-drive motors," *IEEE Trans. Power Electron.*, vol. 15, no. 6, pp. 1056–1064, Nov. 2000.

[23] F. Aghili, "Ripple suppression of BLDC motors with finite driver/amplifer bandwidth at high velocity," *IEEE Trans. Control Syst. Technol.*, vol. PP, no. 99, pp. 1–7, 2010.

[24] H. Lu, L. Zhang, and W. Qu, "A new torque control method for torque ripple minimization of BLDC motors with un-ideal back EMF," *IEEE Trans. Power Electron.*, vol. 23, no. 2, pp. 950–958, Mar. 2008.